# Enhanced acyl-CoA:cholesterol acyltransferase activity increases cholesterol levels on the lipid droplet surface and impairs adipocyte function

Received for publication, September 27, 2019, and in revised form, November 11, 2019 Published, Papers in Press, November 14, 2019, DOI 10.1074/jbc.RA119.011160

**Yanqing Xu**[‡], **Ximing Du**[‡], **Nigel Turner**[§], **Andrew J. Brown**[‡1], **and Hongyuan Yang**[‡2]

*From the Schools of* [‡]*Biotechnology and Biomolecular Sciences and* [§]*Medical Sciences, the University of New South Wales, Sydney, New South Wales 2052, Australia*

Edited by George M. Carman

**Cholesterol plays essential structural and signaling roles in mammalian cells, but too much cholesterol can cause cytotoxicity. Acyl-CoA:cholesterol acyltransferases 1 and 2 (ACAT1/2) convert cholesterol into its storage form, cholesteryl esters, regulating a key step in cellular cholesterol homeostasis. Adipose tissue can store >50% of whole-body cholesterol. Interestingly, however, almost no ACAT activity is present in adipose tissue, and most adipose cholesterol is stored in its free form. We therefore hypothesized that increased cholesterol esterification may have detrimental effects on adipose tissue function. Here, using several approaches, including protein overexpression, quantitative RT-PCR, immunofluorescence, and various biochemical assays, we found that ACAT1 expression is significantly increased in the adipose tissue of the *ob*/*ob* mice. We further demonstrated that ACAT1/2 overexpression partially inhibited the differentiation of 3T3-L1 preadipocytes. In mature adipocytes, increased ACAT activity reduced the size of lipid droplets (LDs) and inhibited lipolysis and insulin signaling. Paradoxically, the amount of free cholesterol increased on the surface of LDs in ACAT1/2-overexpressing adipocytes, accompanied by increased LD localization of caveolin-1. Moreover, cholesterol depletion in adipocytes by treating the cells with cholesterol-deficient media or β-cyclodextrins induced changes in cholesterol distribution that were similar to those caused by ACAT1/2 overexpression. Our results suggest that ACAT1/2 overexpression increases the level of free cholesterol on the LD surface, thereby impeding adipocyte function. These findings provide detailed insights into the role of free cholesterol in LD and adipocyte function and suggest that ACAT inhibitors have potential utility for managing disorders associated with extreme obesity.**

Free cholesterol is a key component of mammalian cell membranes and plays essential structural and signaling roles in mammalian cells. However, too much free cholesterol can cause cellular toxicity (1). Thus, an elaborate system exists to maintain cellular cholesterol homeostasis. Key to this regulation is the SREBP/SCAP machinery, which senses excess cellular free cholesterol and suppresses the expression of the enzymes for cholesterol synthesis, including HMGCR (3-hydroxy-3-methyl-glutaryl-CoA reductase), as well as the low-density lipoprotein receptor for cholesterol uptake (2–5). Excess cholesterol can also trigger the degradation of enzymes for cholesterol synthesis (6, 7). Another crucial biochemical reaction that maintains a proper level of free cholesterol in mammalian cells is cholesterol esterification, which is the synthesis of cholesteryl esters through the formation of an ester linkage between the 3β-OH moiety in free cholesterol and the carboxyl group of a long chain fatty acyl CoA. This reaction is mediated by the enzyme acyl-CoA:cholesterol acyltransferase (ACAT)[3] (also known as sterol *O*-acyltransferase, or SOAT) (8). When in excess, free cholesterol is converted into cholesteryl esters and stored in lipid droplets (LDs), which are dynamic cellular organelles comprising a neutral lipid core enclosed by a phospholipid monolayer (9, 10). Triacylglycerols (TAGs) and cholesteryl esters are two major storage neutral lipids that make up the core of LDs (8, 11). Also, cholesteryl esters can be packaged as part of the neutral lipid core within plasma lipoproteins for lipid transport purposes (12).

There are two acyl-CoA: cholesterol acyltransferases (ACAT1 and ACAT2) in mammals, encoded by the *ACAT1* and *ACAT2* genes, respectively. ACAT1 and ACAT2 are closely related enzymes that are responsible for all intracellular cholesterol esterification (13–15). Both enzymes are membrane-spanning proteins located in the endoplasmic reticulum (ER) (8). ACAT1 is ubiquitously expressed in many cell types, whereas ACAT2 is only expressed in the cells secreting apolipoprotein B–containing lipoproteins, such as the liver and intestine (16–18). It has been shown that cholesterol esterification catalyzed by ACAT2 is essential to cholesterol absorption in the intestine

This work is supported by National Health and Medical Research Council of Australia Project Grants 1141939 and 1144726. The authors declare that they have no conflicts of interest with the contents of this article.

This article contains Tables S1–S4 and Figs. S1–S3.

[1] To whom correspondence may be addressed: School of Biotechnology and Biomolecular Sciences, University of New South Wales, Sydney, NSW, 2052, Australia. Tel.: 61-2-93852005; Fax: 61-2-93851483; E-mail: aj.brown@unsw.edu.au.

[2] Supported by National Health and Medical Research Council Senior Research Fellowship 1058237. To whom correspondence may be addressed: School of Biotechnology and Biomolecular Sciences, University of New South Wales, Sydney, NSW, 2052, Australia. Tel.: 61-2-93858133; Fax: 61-2-93851483; E-mail: h.rob.yang@unsw.edu.au.

[3] The abbreviations used are: ACAT, acyl-CoA:cholesterol acyltransferase; LD, lipid droplet; TAG, triacylglycerol; ER, endoplasmic reticulum; EV, empty vector; PPPA, pyripyropene A; ATGL, adipose triglyceride lipase; HPCD, hydroxypropyl-β-cyclodextrin; HSL, hormone sensitive lipase; LPDS, lipoprotein-deficient serum; DMEM, Dulbecco's modified Eagle's medium; PSG, penicillin/streptomycin/glutamine; PFA, paraformaldehyde.

(19). Adipose tissue is the major storage site of excess calories in the form of TAGs in mammals (20). It also contains the largest pool of free cholesterol in the body (21, 22). In obese subjects, over 50% of total body cholesterol resides in the adipose tissue (21). We have recently demonstrated a major contribution of adipose tissue to the storage of whole-body cholesterol (23). Because of a lack of ACAT enzyme activity in white adipose tissue, nearly all cholesterol (> 95%) exists in its free form (24). Most free cholesterol in adipocytes is believed to localize to the plasma membrane, where there are abundant caveolae, small flask-shaped invaginations that are highly enriched in free cholesterol (25, 26). The activity of *de novo* cholesterol biosynthesis in adipocytes is fairly low (21). Therefore, much of the adipocyte cholesterol is obtained through the uptake of circulating lipoproteins.

Given that a large quantity of cholesterol is stored in adipose tissue, the absence of ACAT expression and activity in adipose tissue is intriguing. As mentioned above, excess free cholesterol is toxic, and the best way to handle excess cholesterol is to convert it into cholesteryl esters, which can be stored in the core of LDs. What are the benefits, then, for adipocytes to maintain low ACAT expression and activity? In this study, we first detected significantly increased level of ACAT1 in the adipose tissue/adipocytes of *ob*/*ob* mice. We further investigated the effects of increased cholesterol esterification on adipocyte function and LD dynamics by overexpressing ACAT1/2 in pre- and mature adipocytes. Our data demonstrated that increased ACAT activity partially blocked adipogenesis, caused dramatic enrichment of free cholesterol on the LD surface, and impaired key functions of adipocytes including lipolysis and insulin signaling.

## Results

### *ACAT1/2 overexpression in 3T3-L1 stable cell lines*

Because normal adipose tissue maintains very low ACAT expression and activity, we suspect that increased ACAT expression/activity may exert adverse effects on adipose function and may also be associated with dysfunctional adipose tissue. Indeed, we found that the protein level of ACAT1 was ~7-fold higher in the adipose tissue of the *ob*/*ob* mice than that of the WT mice (Fig. 1, *A* and *B*). Given that *ob*/*ob* adipose tissue has very high levels of macrophages and that macrophages are known to express ACAT1 (27), the detected ACAT1 on whole adipose tissue could be derived from adipose tissue macrophages. We therefore isolated adipocytes: ACAT1 was detected in isolated adipocytes from the *ob*/*ob* mice but not WT mice (Fig. S1*A*). By contrast, the macrophage marker CD11b was detected only in the stromal vascular fraction, but not in isolated adipocytes. Thus, the increase in adipose tissue ACAT1 is at least in part due to increased ACAT1 in adipocytes of the *ob*/*ob* mice. Thus, it is important to determine whether and how increased ACAT activity may impact adipocyte function. For this purpose, we generated stable cell lines (3T3-L1) overexpressing FLAG-tagged ACAT1/2, an ACAT2 stabilizing mutant (ACAT2-C277A) (28), and their catalytic dead mutants (ACAT1-H460A, ACAT2-H360A, and ACAT2-H360A-C277A). For both WT and mutants of ACAT1 and ACAT2, the mRNA levels of *ACAT1* or *ACAT2* were increased by at least 3 orders of magnitude above endogenous levels in the empty vector (EV) control group (Fig. 1*C*). Accordingly, protein levels of ACAT1 and ACAT2 were also much higher in these overexpressing cell lines (Fig. 1, *D* and *E*), with the level of the ACAT2 stable mutant, ACAT2-C277A, ~5-fold higher than the WT (Fig. S1, *B* and *C*). In both 3T3-L1 preadipocytes (Fig. 1*F*) and differentiated 3T3-L1 adipocytes (Fig. 1*G*), total cholesteryl esters were significantly higher than that of control/EV cells when overexpressing ACAT1, ACAT2, and ACAT2-C277A, but not the catalytic dead mutants. The proportion of total cholesterol that was converted to cholesteryl esters was shown in Fig. 1 (*H* and *I*). Finally, the enzymatic activity of the ACATs was determined by a cholesterol esterification assay in which those stable cells were pulse-labeled with [$^{14}$C]oleic acid conjugated to BSA. Although WT ACAT1/2 and the ACAT2 stabilizing mutant (ACAT2-C277A) demonstrated significantly higher activities, the catalytic dead mutants appeared to be inactive (Fig. 1, *J* and *K*). Therefore, our 3T3-L1 stable cell lines were shown to overexpress functional ACAT1/2 with the catalytic dead mutants serving as useful controls.

### *Increased ACAT activity impairs the differentiation of 3T3-L1 preadipocytes*

The effects of ACAT1/2 on adipogenesis were investigated by differentiating 3T3-L1 preadipocytes into mature adipocytes using our stable cell lines. The mRNA levels of adipose-specific genes, such as *aP2*, *PPARγ*, and *C/EBPα*, are up-regulated in normal adipocytes, whereas *Prefl* is mainly expressed in preadipocytes (29–31). Thus, the expression of *aP2*, *PPARγ*, and *C/EBPα* was induced during differentiation (day 8 *versus* day 0), whereas that of *Pref1* was down-regulated (Fig. 2*A*). However, after 8 days of differentiation, overexpression of functional ACAT1/2 blunted the changes in these differentiation markers. Overexpression of ACAT2 and ACAT2-C277A decreased the extent of differentiation by ~70% (Fig. 2, *A* and *B*), whereas the catalytic dead mutants had little or much weaker effects on differentiation (Fig. 2*C*). These results were reflected by reduced triglyceride accumulation as assessed by Oil Red O staining (Fig. 2*D*), with catalytic dead mutants serving as controls (Fig. 2*E*). Together, these data suggest that ACAT expression negatively impacts the differentiation of 3T3-L1 cells.

### *ACAT1/2 overexpression impairs lipid droplet morphology in adipocytes*

Lipid droplets form during adipocyte differentiation/adipogenesis. We next examined the morphology of lipid droplets in mature adipocytes. ACAT1/2 overexpression, especially ACAT2, substantially reduced the LD size in adipocytes on day 8 after differentiation (Fig. 3, *A* and *C*, and Fig. S2*A*). The size of LDs also decreased in adipocytes on day 0 and 2, as well as in HeLa cell lines upon ACAT1/2 overexpression (Fig. S2, *B–D*). Catalytic dead mutants of ACAT1 and ACAT2 did not affect the LD size (Fig. 3, *B* and *C*). To exclude the possibility that the impaired LD size was related to the differentiation status, we additionally investigated the lipid droplet growth in mature adipocytes transduced by lentivirus carrying the *ACAT1* or

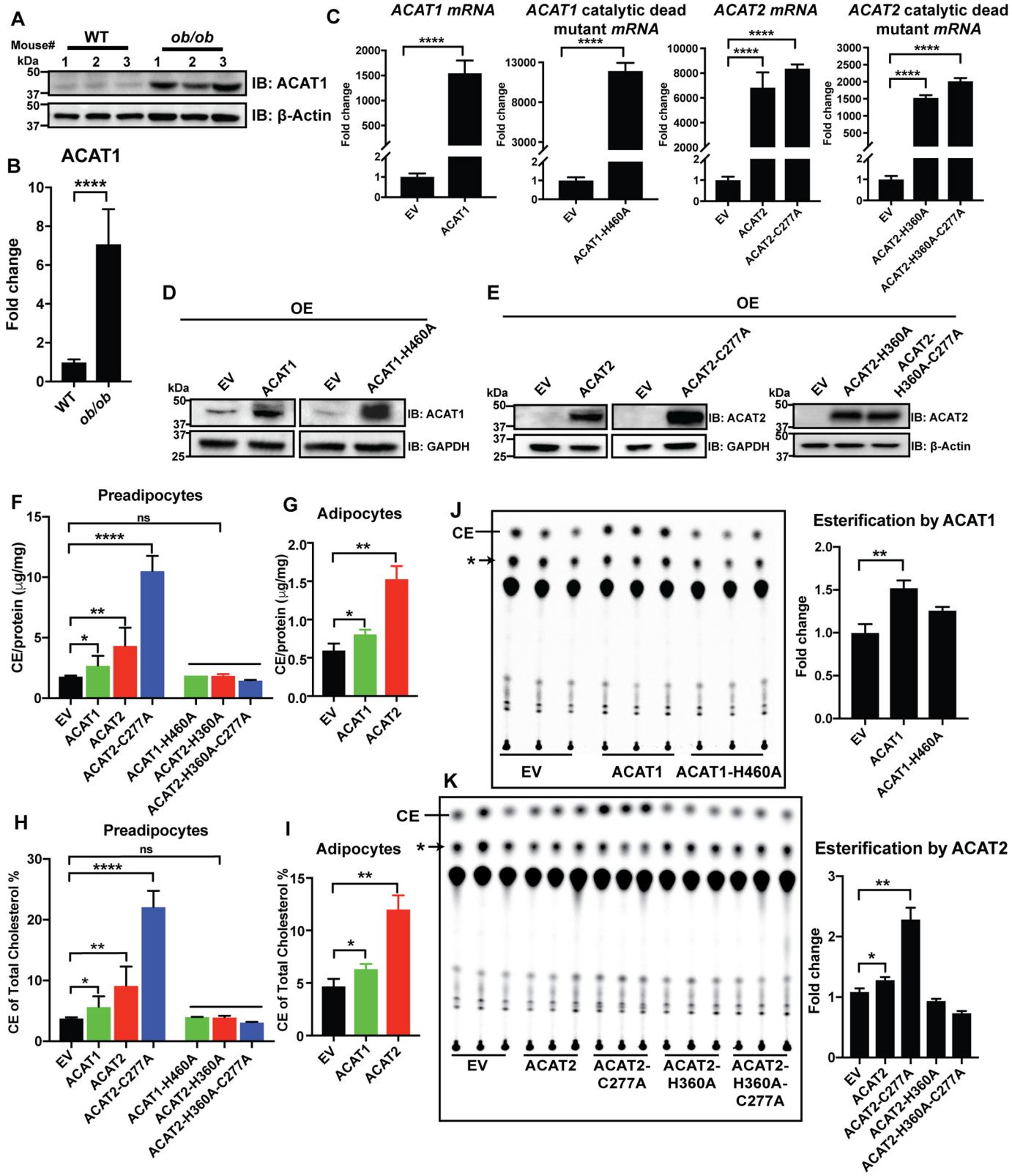


**Figure 1. Characterization of ACAT1/2 overexpression in 3T3-L1 stable cells.** *A*, the protein level of ACAT1 in adipose tissue of WT and *ob*/*ob* mice (three mice for each genotype, male, 18–20 weeks) as detected by Western blotting analyses. *B*, quantification of ACAT1 levels in *A*. *C*, the mRNA levels of ACAT1, ACAT2, and related mutants stably expressed in 3T3-L1 adipocytes. *D* and *E*, the protein levels of ACAT1, ACAT2, and related mutants stably expressed in 3T3-L1 adipocytes. *OE*, overexpression. *F* and *G*, the levels of cholesteryl esters (*CE*) in preadipocytes and adipocytes. *H* and *I*, the proportion of esterified cholesterol over total cholesterol. *J* and *K*, cholesterol esterification by ACAT1 and ACAT2 in preadipocytes. Nonspecific lipids (*) were used as references for normalization. 3T3-L1 preadipocytes were transduced with pBABE-puro EV or FLAG-tagged ACAT1/2 or ACAT1/2 catalytic dead mutants followed by the selection of puromycin to generate stable cell lines. Two-tailed Student's *t* test was used (means ± S.D.; $n = 3$). *, $p < 0.05$; **, $p < 0.01$; ****, $p < 0.0001$; *ns*, no significance.

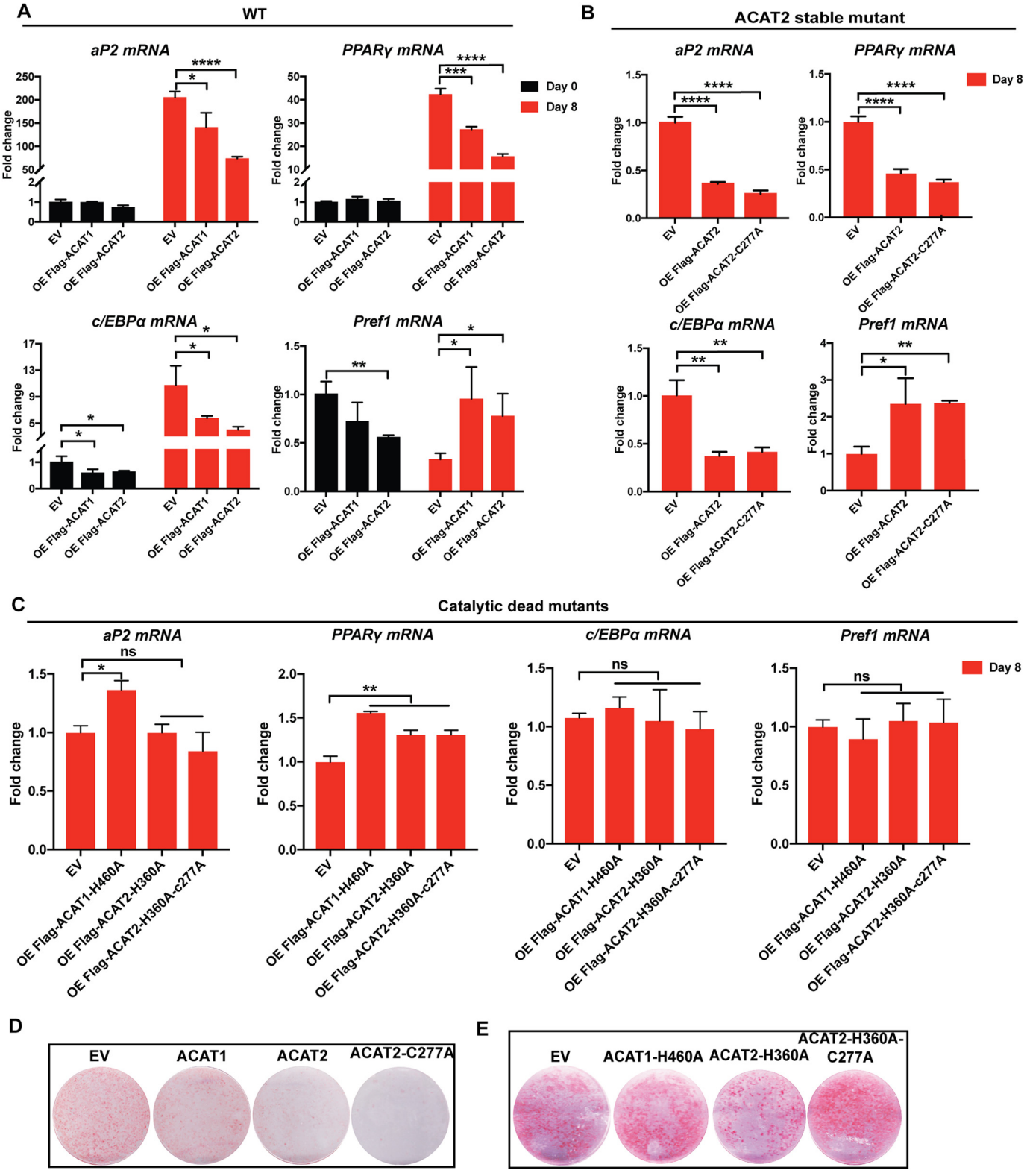


**Figure 2. ACAT1/2 overexpression impaired 3T3-L1 differentiation.** *A–C*, the mRNA levels of *aP2*, *PPARγ*, *C/EBPα*, and *Pref1* during differentiation. The status of differentiation was assayed by examining the mRNA levels of adipose-specific genes when overexpressing WT ACAT1 and ACAT2 (*A*), stable mutant of ACAT2 (ACAT2-C277A) (*B*), and catalytic dead mutants of ACAT1/2 (*C*). *D* and *E*, Oil red O staining of adipocytes on day 8 of differentiation. Two-tailed Student's *t* test was used (means ± S.D.; $n = 3$). *, $p < 0.05$; **, $p < 0.01$; ***, $p < 0.001$; ****, $p < 0.0001$; *ns*, no significance.

*ACAT2* genes, respectively (Fig. 3, *D* and *E*), and obtained consistent results that the presence of ACATs in mature adipocytes, especially ACAT2, reduced LD growth (Fig. 3, *F* and *G*). Importantly, this effect can be reversed by inhibiting ACAT1 with Sandoz 58-035 and ACAT2 with pyripyropene A (PPPA), respectively (Fig. 3, *H* and *I*).

CIDEC/Fsp27 is a well-known LD-associated protein. Although very low in preadipocytes, the expression of CIDEC is highly induced during differentiation to regulate lipid droplet dynamics in adipocytes (32–34). Hence, we examined the expression of CIDEC in mature adipocytes when overexpressing ACAT1/2. Overexpression of ACAT1/2 dramatically decreased the CIDEC expression in total cell lysates and LD fractions in mature adipocytes (Fig. 3, *J* and *K*), which implied

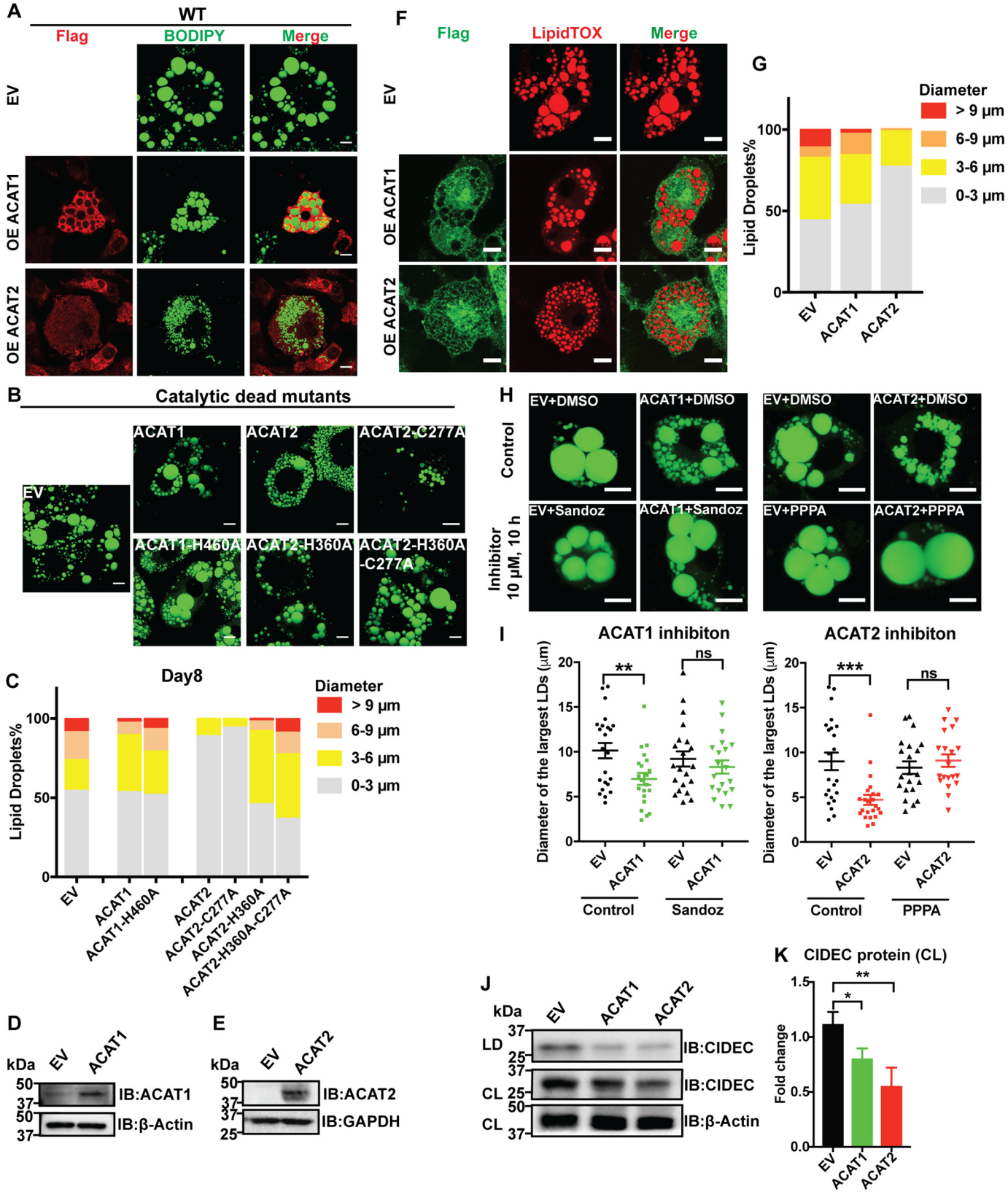

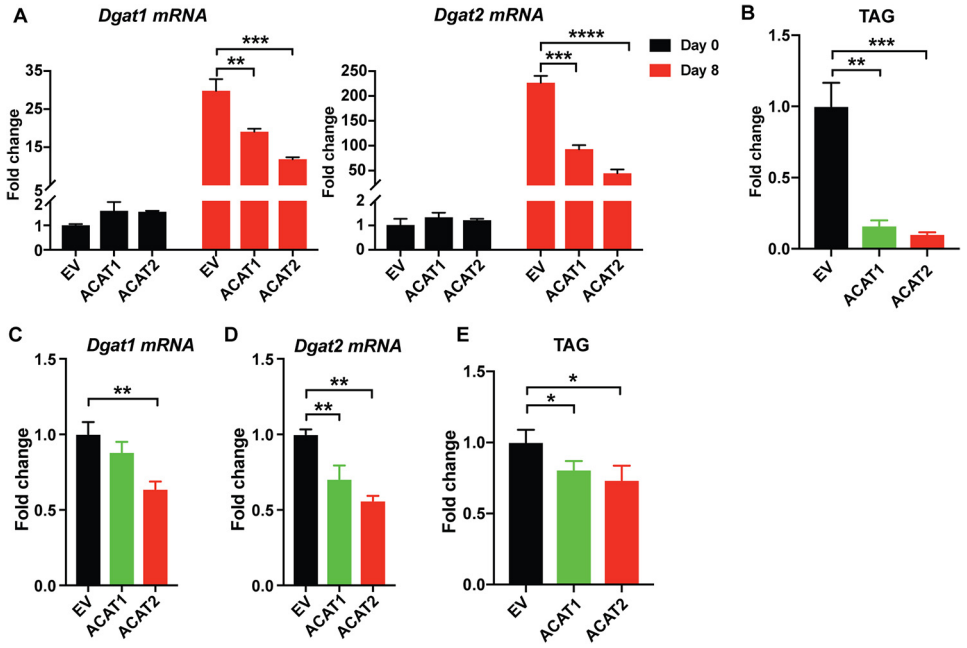


**Figure 4. ACAT1/2 overexpression impaired TAG synthesis in adipocytes.** *A*, the mRNA level of *Dgat1/2* during differentiation. *B*, the amount of TAG in adipocytes on day 8 of differentiation. *C* and *D*, the mRNA level of *Dgat1/2* in mature adipocytes transiently overexpressing ACAT1 and ACAT2. *E*, the amount of TAG in mature adipocytes overexpressing ACAT1 and ACAT2. Two-tailed Student's *t* test was used (means ± S.D.; $n = 3$). *, $p < 0.05$; **, $p < 0.01$; ***, $p < 0.001$; ****, $p < 0.0001$.

that increased ACAT activity in adipocytes may influence LD-associated proteins and disturb LD dynamics.

LDs are composed of a core of neutral lipids, including cholesteryl esters produced by ACAT1/2 and TAGs produced by DGAT1 and DGAT2 (11, 35, 36). The impaired LD size when overexpressing ACATs may also be related to TAG synthesis. Therefore, we examined TAG synthesis in adipocytes in the presence of ACAT1/2. The mRNA level of *Dgat1* or *Dgat2* was significantly reduced on day 8 of differentiation (Fig. 4*A*), with concomitant dramatically reduced TAG production (Fig. 4*B*). Also, we found consistent results in mature adipocytes transiently overexpressing ACAT1 or ACAT2 (Fig. 4, *C–E*). Taken together, these data suggest that ACAT1/2 overexpression impairs LD expansion in adipocytes, possibly because of less LD fusion mediated by CIDEC and down-regulated TAG synthesis.

### *ACAT1/2 overexpression impairs lipolysis and insulin signaling in adipocytes*

The dramatic changes in LD morphology in adipocytes upon ACAT1/2 overexpression may impact adipocyte functions. First, we investigated lipolysis in mature adipocytes transiently overexpressing ACAT1/2. ACAT1/2 overexpression almost abolished hormone-stimulated lipolysis in mature adipocytes (Fig. 5*A*). Perilipin is a key regulator for lipolysis and regulates lipases such as hormone-sensitive lipase (HSL) and adipose triglyceride lipase (ATGL) (37, 38). Phosphorylated forms of HSL were clearly reduced in mature adipocytes transiently overexpressing ACAT1/2 (Fig. 5*B*). In addition to perilipin 1, perilipin 2 expression was also significantly reduced in mature adipocytes upon overexpressing ACAT2 (Fig. 5, *C* and *D*). This effect was much stronger in stable cell lines, where ACAT1 overexpression also dramatically reduced perilipin 2 expression (Fig. 5, *E* and *F*). No changes were detected in the expression of ATGL (Fig. 5, *C–F*).

Insulin triggers the uptake of glucose, fatty acids, and amino acids in the liver, adipose tissue, and muscle and promotes the storage of these nutrients in the form of glycogen, lipids, and protein, respectively (39, 40). Protein kinase B (AKT), a downstream target of insulin, is one of the important regulators during this process. ACAT1/2 overexpression substantially decreased the level of p-AKT (S473), with ACAT2 overexpression displaying a stronger effect (Fig. 5, *G* and *H*). All these results strongly indicate that increased ACAT activity severely disrupts the metabolic functions of mature adipocytes.

**Figure 3. ACAT1/2 overexpression impaired LD expansion in adipocytes.** *A*, the effect of WT ACAT1/2 overexpression on LD sizes on day 8 of differentiation. Immunofluorescence was carried out with anti-FLAG primary antibody on cells expressing FLAG-tagged ACAT1/2, but not on EV control cells. LDs were stained using BODIPY. *Bars*, 10 μm. *B*, the effect of overexpressing catalytic dead mutants of ACAT1/2 on LD size on day 8 of differentiation. LDs were stained using BODIPY. *Bars*, 10 μm. *C*, quantification of LD sizes in adipocytes stably expressing ACAT1/2. LDs from ~15 cells/cell type were used. *D*, protein level of ACAT1 in mature adipocytes transiently overexpressing ACAT1. *E*, protein level of ACAT2 in mature adipocytes transiently overexpressing ACAT2. *F*, the effect of transient overexpression of ACAT1/2 on LD size in mature adipocytes. Immunofluorescence was carried out with anti-FLAG primary antibody on cells expressing FLAG-tagged ACAT1/2, but not on EV control cells. LDs were stained using LipidTOX. *Bars*, 10 μm. *G*, quantification of LD sizes in mature adipocytes overexpressing ACAT1/2. LDs from ~15 cells/cell type were used. *H*, the effects of ACAT1 and ACAT2 inhibitors on LD size in mature adipocytes. *Bars*, 10 μm. LDs were stained by BODIPY. Sandoz 58-035 (ACAT1 inhibitor) and PPPA (ACAT2 inhibitor) were dissolved in DMSO. 10 μM of inhibitor was added to respective cells for 10 h. *I*, quantification of diameters of 2 largest LDs in each cell type as shown in *H*. Two-tailed Student's *t* test was used (means ± S.E.; $n = 20$ LDs from 10 cells for each cell type). **, $p < 0.01$; ***, $p < 0.01$; *ns*, no significance. *J*, immunoblot (*IB*) analysis of CIDEC in cell lysates (*CL*) and LD fractions isolated from mature adipocytes transiently overexpressing ACAT1/2. *K*, quantification of CIDEC level in *J*. Two-tailed Student's *t* test was used (means ± S.D.; $n = 3$). *, $p < 0.05$; **, $p < 0.01$.

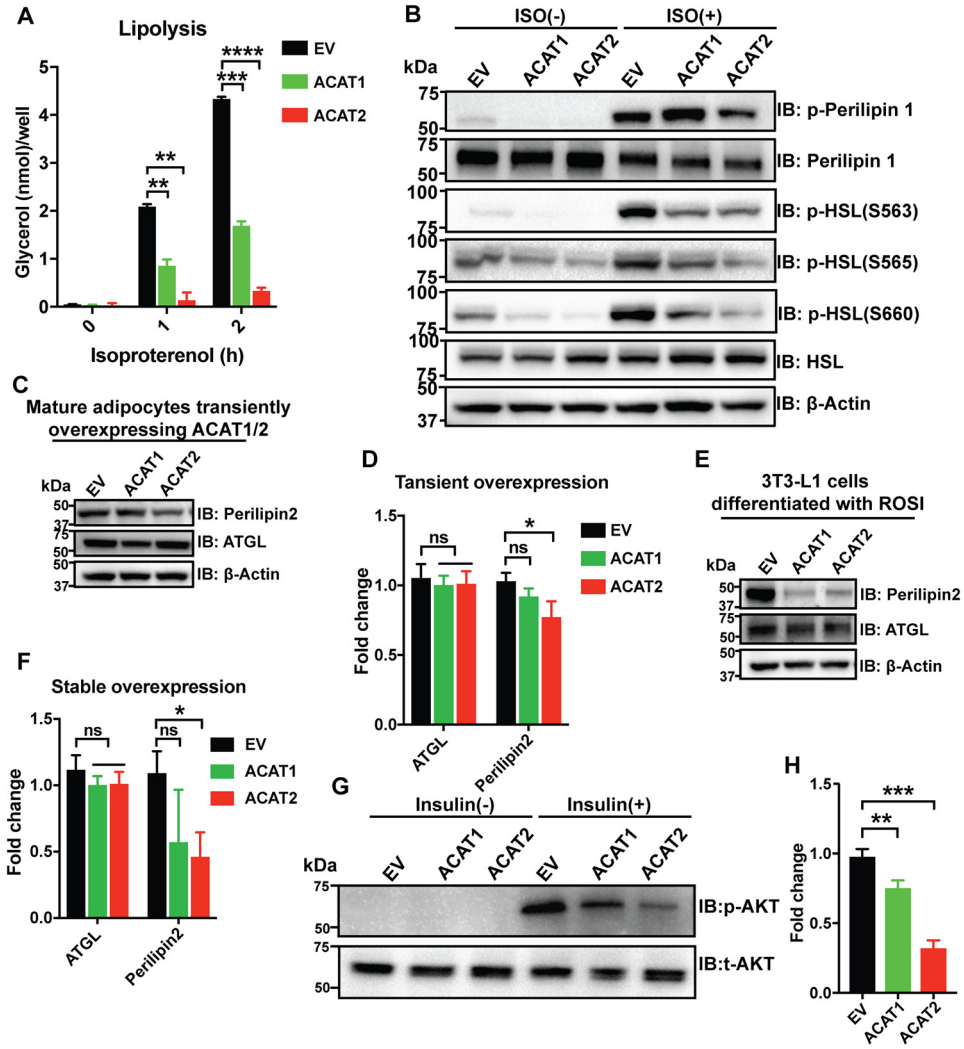


**Figure 5. ACAT1/2 overexpression impaired metabolic functions in adipocytes.** *A*, lipolysis assay in mature adipocytes overexpressing ACAT1/2. 100 nM isoproterenol was used. Two-tailed Student's *t* test was used (means ± S.D.; $n = 3$). **, $p < 0.01$; ***, $p < 0.001$; ****, $p < 0.0001$. *B*, immunoblot (*IB*) analysis of p-perilipin 1 (Ser$^{522}$) and p-HSL (Ser$^{660}$) in mature adipocytes transiently overexpressing ACAT1/2. *ISO*, isoproterenol, 10 μM, 2 h. *C*, immunoblot analysis of perilipin 2 and ATGL in mature adipocytes overexpressing ACAT1/2. *D*, quantification of perilipin2 and ATGL levels in *C*. Two-tailed Student's *t* test was used (means ± S.D.; $n = 3$). *, $p < 0.05$; *ns*, no significance. *E*, immunoblot analysis of perilipin 2 and ATGL in mature adipocytes stably overexpressing ACAT1/2. *F*, quantification of perilipin2 and ATGL levels in *E*. Two-tailed Student's *t* test was used (means ± S.D.; $n = 3$). *, $p < 0.05$; *ns*, no significance. *G*, immunoblot analysis of p-AKT (Ser$^{473}$) in mature adipocytes stably overexpressing ACAT1/2. 10 nM insulin was added to cells for 15 min. *H*, quantification of p-AKT level in *G*. Two-tailed Student's *t* test was used (means ± S.D.; $n = 3$). **, $p < 0.01$; ***, $p < 0.001$.

### *ACAT1/2 overexpression promotes free cholesterol accumulation on lipid droplets in adipocytes*

Next, we wanted to understand the molecular basis underlying the impact of ACAT expression on adipocytes. We focused on cholesterol, the substrate of ACAT enzymes and a key component of mammalian membranes. Strikingly, as revealed by filipin staining, there was appreciable free cholesterol accumulating on the LD surface instead of the plasma membrane when overexpressing ACAT1/2 in adipocytes on day 8 after differentiation, and ACAT2 overexpression showed stronger effects (Fig. 6, *A* and *B*). Moreover, this phenotype was also seen in mature adipocytes transiently overexpressing ACAT1 or ACAT2, respectively (Fig. 6, *C* and *D*). The biosynthesis of cholesterol is sensitive to the level of free sterols, the feedback of which elaborately regulates the endogenous synthesis and exogenous uptake of cholesterol. ACAT1/2 in adipocytes consumes free cholesterol, which may reduce the cholesterol sensing "pool" in the ER, thereby triggering the ER to keep producing cholesterol, leading to free cholesterol accumulation on lipid droplets. To test this hypothesis, two other approaches of depleting cholesterol were carried out in mature adipocytes: using hydroxypropyl-β-cyclodextrin (HPCD) and/or starvation medium (DMEM + 1% lipoprotein-deficient serum (LPDS)). The depletion of cholesterol enhanced the accumulation of free cholesterol on the LD surface (Fig. 7). Striking accumulation of free cholesterol on the LD surface could be observed even in control cells when depleting cholesterol using HPCD (Fig. 7, *A* and *C*) or shutting down cholesterol uptake (LPDS medium) (Fig. 7, *B* and *C*).

Caveolin-1 is a free cholesterol-binding protein and required for cholesterol homeostasis, maintenance, and distribution (41–45). Caveolin-1 colocalized with free cholesterol on the LD surface in mature adipocytes upon overexpression of ACAT1 and especially ACAT2 (Fig. 8*A*). The protein level of caveolin-1

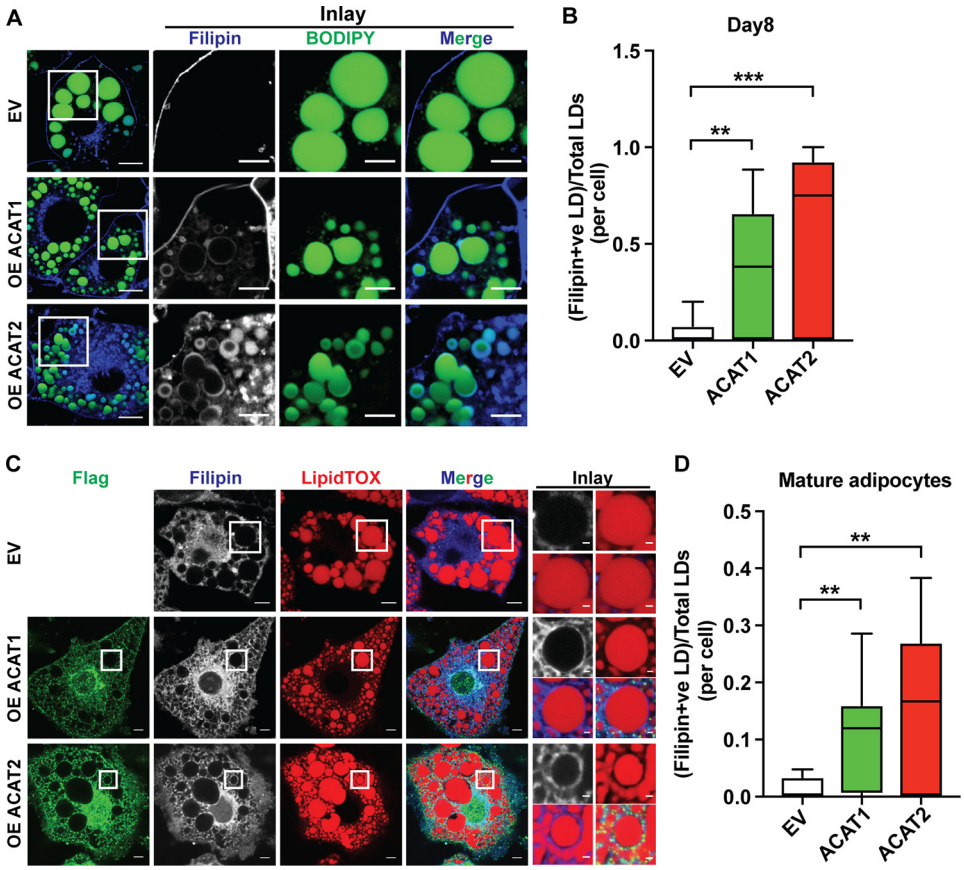


**Figure 6. ACAT1/2 overexpression resulted in accumulation of free cholesterol on the LD surface in adipocytes.** *A*, the localization of free cholesterol in adipocytes on day 8 of differentiation upon ACAT1/2 overexpression. *Bars*, 10 $\mu$m. *Inset*, *bars*, 5 $\mu$m. *B*, quantification of free cholesterol-LD colocalization in *A*. Two-tailed Student's *t* test was used (minimum to maximum, line at median; $n = 15$ cells). **, $p < 0.01$; ***, $p < 0.001$. *C*, the localization of free cholesterol in mature adipocytes transiently overexpressing ACAT1/2. Immunofluorescence was carried out with anti-FLAG primary antibody on cells expressing FLAG-tagged ACAT1/2, but not on EV control cells. *Bars*, 10 $\mu$m. *Inset*, *bars*, 1 $\mu$m. *D*, quantification of free cholesterol-LD colocalization in *C*. Two-tailed Student's *t* test was used (minimum to maximum, line at median; $n = 10$ cells). **, $p < 0.01$.

in the presence of ACAT1/2 was increased either in total cell lysates or LD fractions isolated from mature adipocytes (Fig. 8, *B* and *C*). In summary, our results showed that the overexpression of ACAT1/2 in 3T3-L1 adipocytes perturbs cholesterol transport and localization, promoting cholesterol accumulation on the LD surface.

### *ACAT1/2 overexpression impairs cholesterol homeostasis in adipocytes*

We next sought to investigate cholesterol status and homeostasis in mature adipocytes when ACAT1/2 are overexpressed. The free cholesterol level was significantly increased in mature adipocytes that were differentiated from 3T3-L1 preadipocytes stably overexpressing ACAT1/2 (Fig. 9*A*), as well as mature adipocytes transiently overexpressing ACAT1/2 (Fig. 9*C*) compared with control cells. Accordingly, increased free cholesterol was associated with the down-regulation of *Hmgcr* (Fig. 9, *B* and *D*), an SREBP-target gene that is sensitive to changes in cellular cholesterol status. Consistent results were also found in preadipocytes stably overexpressing ACAT1/2 (Fig. 9, *E* and *F*). Although overexpression of WT ACAT1/2 or ACAT2 stable mutant increased free cholesterol levels, the catalytic dead mutants of ACAT1/2 had no effects (Fig. 9, *E* and *F*). Furthermore, the increased free cholesterol could be reversed through inhibiting HMGCR activity by statin treatment (Fig. 9, *G* and *H*). Together, these results indicate that ACAT overexpression perturbs cholesterol homeostasis in adipocytes.

## Discussion

Adipose tissue can store more than 50% of whole-body cholesterol. Our previous study demonstrated that mice deficient in both LDLR and adipose tissue had ~5-fold higher plasma cholesterol than $Ldlr^{-/-}$ mice (23). Thus, adipose tissue is just as important as the LDLR pathway for whole body cholesterol homeostasis. Cholesterol is usually stored in cells in the form of cholesterol esters through the actions of ACAT1/2. However, ACAT1/2 expression and activity are extremely low in normal adipocytes, which is highly intriguing. We hypothesize that increased ACAT expression/activity may exert adverse effects on adipose function and may also be associated with dysfunctional adipose tissue. Indeed, we show here for the first time that ACAT1 is dramatically up-regulated in the adipose tissue and adipocytes of the *ob*/*ob* mice (Fig. 1, *A* and *B*, and Fig. S1*A*). Thus, it is important to determine whether and how increased ACAT activity may negatively impact adipocyte function. In this work, we demonstrated that the overexpression of ACAT1/2 impaired adipogenesis and key metabolic functions of mature adipocytes. We further demonstrate that overexpressing ACAT1/2 caused striking accumulation of free cholesterol on the surface of LDs, as well as an overall increase in

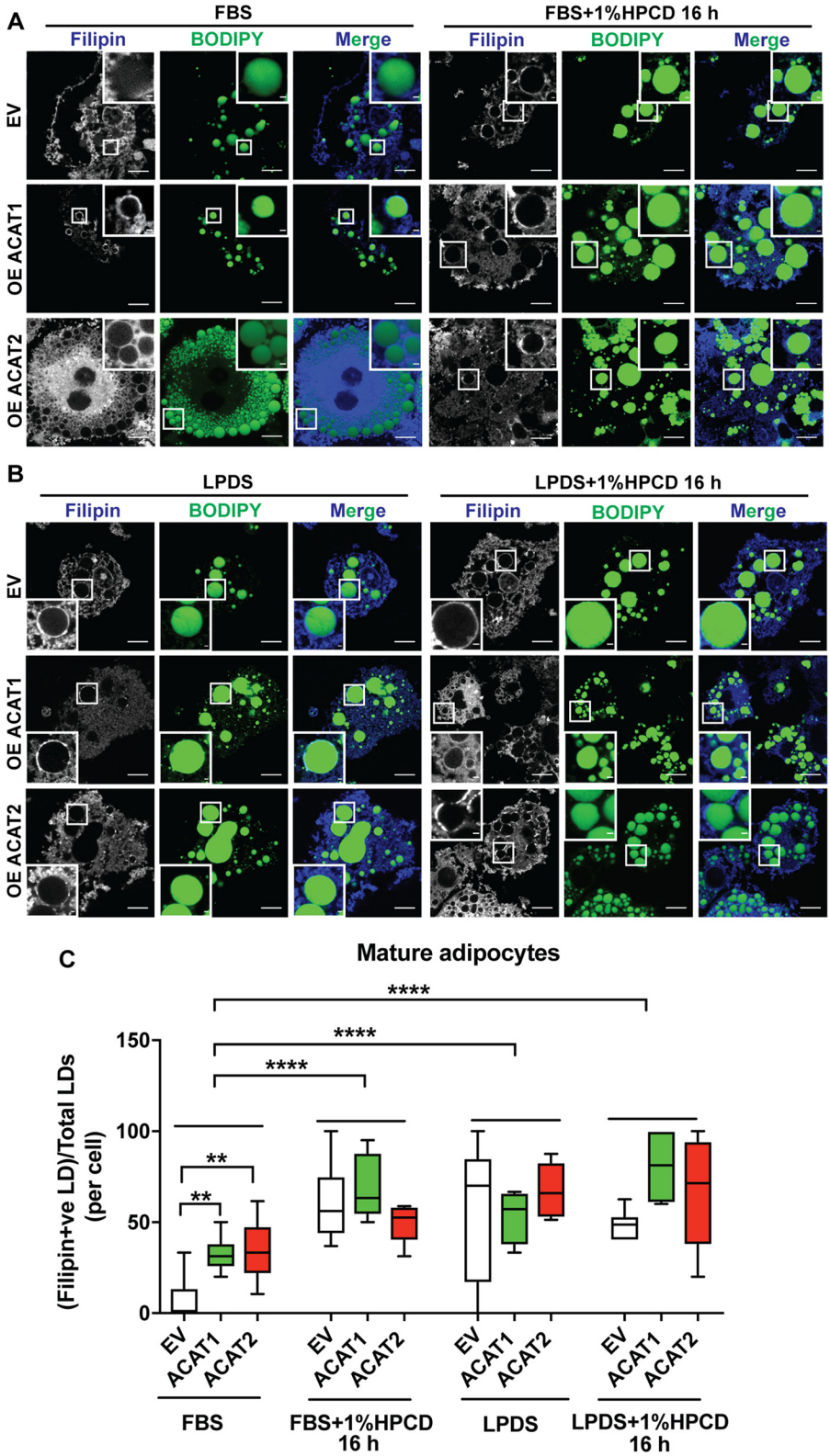


**Figure 7. Cholesterol depletion enhanced free cholesterol accumulation on LD surface in adipocytes.** *A* and *B*, cholesterol depletion by HPCD in FBS medium (*A*) and HPCD in LPDS medium (*B*) promoted free cholesterol accumulation on the LD surface in mature adipocytes stably overexpressing ACAT1/2. *Bars*, 10 $\mu$m. *Inset*, *bars*, 1 $\mu$m. *C*, quantification of free cholesterol-LD colocalization in *A* and *B*. One-way analysis of variance was used (minimum to maximum, line at median; $n = 10$ cells). **, $p < 0.01$; ****, $p < 0.0001$.

cellular free cholesterol. Thus, the adverse metabolic effects on adipocytes may arise from dysregulated cellular cholesterol homeostasis upon increased ACAT activity.

Adipose tissue stores a large amount of free cholesterol because of a relative deficiency of ACAT enzymes. However, what little cholesterol esterifying activity remains in adipocytes still contrib-

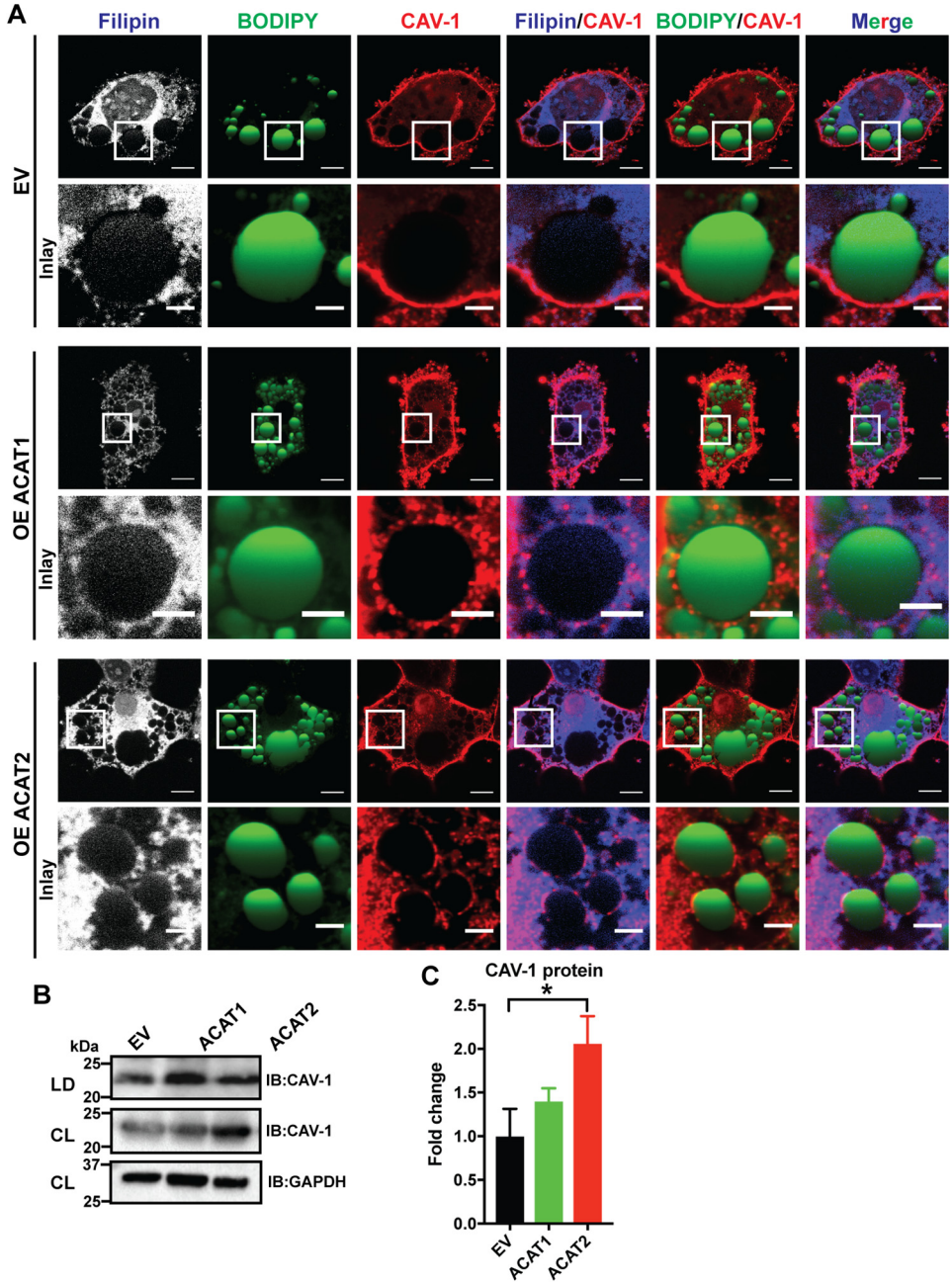


**Figure 8. ACAT1/2 overexpression promoted caveolin-1 localization to the LDs in adipocytes.** *A*, caveolin-1 colocalized with free cholesterol on the LD surface in mature adipocytes upon ACAT1/2 overexpression. *Bars*, 10 $\mu$m. *Inset*, *bars*, 3 $\mu$m. *CAV-1*, caveolin-1. *B*, immunoblot analysis of caveolin-1 in LD fractions isolated from mature adipocytes transiently overexpressing ACAT1/2. *CL*, cell lysates. *C*, quantification of caveolin-1 level in *B*. Two-tailed Student's *t* test was used (means $\pm$ S.D.; $n = 3$). *, $p < 0.05$.

utes to adipocyte function, because ACAT inhibition and *ACAT* deficiency have been reported to suppress lipogenesis and reduce the intracellular cholesterol pool (46). Here we found that ACAT overexpression reduced TAG synthesis and yet increased intracellular cholesterol, thus transgressing the strong correlation usually observed between adipocyte cholesterol content and TAG load (22). ACAT overexpression led to smaller LDs (Fig. 3, *C* and *G*), and hence too much ACAT could be expected to inhibit the formation of the adipocyte's characteristic unilocular LDs, which helps to maximize energy storage in minimal space.

ACAT2 appeared to display stronger effects than that of ACAT1, which may help to explain its far more restricted tissue expression. ACAT2 expression is mostly limited to the intestine and liver where it helps to package cholesteryl esters into apolipoprotein B–containing lipoproteins (47–49). Accordingly, endogenous ACAT2 was down-regulated during adipocyte differentiation unlike ACAT1 (Fig. S3 and Table S4). Moreover, we did not detect any difference in the protein level of ACAT2 between the adipose tissue of normal and *ob*/*ob* mice (data not shown), further confirming ACAT2's tissue specificity.

$Cys^{277}$ of ACAT2 can be ubiquitinated for degradation when the level of certain lipids is low. Free cholesterol and saturated free fatty acids can protect the protein from degradation

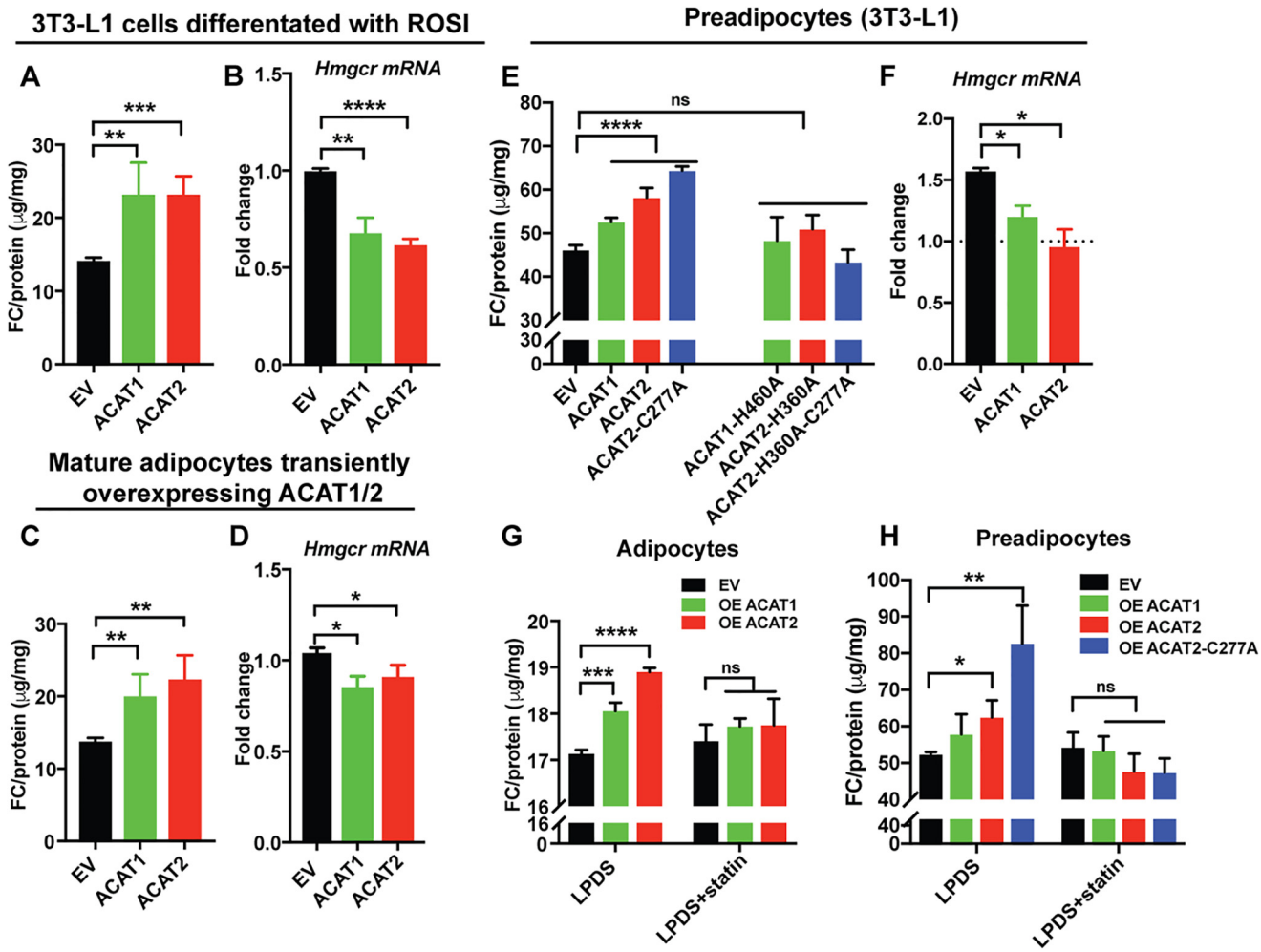


**Figure 9. ACAT1/2 overexpression impaired cholesterol homeostasis in adipocytes.** *A* and *B*, the level of free cholesterol (*FC*) (*A*) and the mRNA level of *Hmgcr* in (*B*) mature adipocytes stably overexpressing ACAT1/2. *ROSI*, rosiglitazone. *C* and *D*, the free cholesterol level (*C*) and the mRNA level of *Hmgcr* (*D*) in mature adipocytes transiently overexpressing ACAT1/2. *E* and *F*, the free cholesterol level (*E*) and the mRNA level of *Hmgcr* (*F*) in preadipocytes stably overexpressing ACAT1 and ACAT2. 200 $\mu$M oleate was added to cells for 20 h before harvest. *G* and *H*, HMGCR inhibition restored the free cholesterol level in preadipocytes and adipocytes stably overexpressing ACAT1 and ACAT2. Before harvest, the cells were washed once with PBS followed by the treatment of LPDS medium for 20 h. For preadipocytes, 200 $\mu$M oleate was added to cells with LPDS medium to induce LDs for 20 h. Two-tailed Student's *t* test was used (means ± S.D.; $n = 3$). *, $p < 0.05$; **, $p < 0.01$; ***, $p < 0.001$; ****, $p < 0.0001$; *ns*, no significance.

through inducing cellular reactive oxygen species to oxidize $Cys^{277}$ (28). This may be another reason for the absence of ACAT2 in adipose tissue that stores the most lipids, including free cholesterol and free fatty acids. Cysteine ubiquitination of ACAT2 is believed to be an important mechanism of maintaining lipid homeostasis by sensing lipid overload. A stable mutant of ACAT2 (C277A) caused higher insulin sensitivity in the liver of *Acat2* KO mice (28). In addition to ACAT2, the stability of HMGCR is also sensitively regulated by lipid levels (6). The sterol-induced degradation of both ACAT2 and HMGCR is accomplished through the same gp78–Insigs complex. Gp78 is a membrane-anchored ubiquitin ligase and associates with Insig1/2. Both ACAT2 and HMGCR are substrates of gp78 (50–53). When the cellular cholesterol is low, the gp78–Insig complex would release and stabilize HMGCR to increase cholesterol synthesis and, at the same time, ubiquitinate $Cys^{277}$ of ACAT2 to reduce the esterification. This may be related to the finding in Fig. 9. In ACAT2-overexpressing cells, the continuous consumption of free cholesterol may inhibit HMGCR degradation and increase cholesterol synthesis, which in time reversibly inhibits *Hmgcr* transcription.

ACAT1/2 expression in adipocytes perturbed cholesterol homeostasis and resulted in an aberrant accumulation of free cholesterol on lipid droplets (Figs. 6 and 9). Cholesterol is synthesized in the ER and quickly transferred to other organelles, especially the plasma membrane. However, the molecular mechanism of this transport is still elusive despite some discoveries (54–56). Our lab recently demonstrated that ORP2 is a coexchanger of cholesterol and $PI(4,5)P_2$ on the plasma membrane (57). Also, ORP2 might regulate cholesterol on the LDs (58). This implies ORP2 might be involved in the cholesterol transport in adipocytes when overexpressing ACAT1/2, which may be tested in future studies. In addition, cholesterol depletion by methyl-$\beta$-cyclodextrin (similar to HPCD used in this study) increased caveolin-1 content in lipid droplets, and *Caveolin-1* KO mice showed reduced free cholesterol level on LDs (43). The association of caveolin-1 and cholesterol in adipocyte lipid droplets implies that caveolin-1 may play an impor-

tant role in the aberrant accumulation of free cholesterol on lipid droplets when expressing ACAT1/2 (Fig. 8). Indeed, the redistribution of caveolin-1 to LDs has been proposed to divert free cholesterol from other intracellular pools (43). Thus, overexpressing ACAT1/2 may limit cholesterol availability for proper caveolae function at the plasma membrane, causing adipocyte dysfunction.

Perilipin and CIDEC/Fsp27 are two key LD-associated proteins in adipocytes for regulating lipolysis and lipid dynamics, respectively. Cholesterol accumulating on LDs when ACAT1/2 are overexpressed may interfere with the localization of perilipin on LDs, thereby affecting lipolysis. Also, it may affect the functions of other lipid droplet-associated proteins such as CIDEC (Fig. 3*J*), DGAT2 (Fig. 4, *A* and *D*), and HSL (Fig. 5). All the perturbations in adipocytes caused by increased esterification seem to be associated with the proteins coating the LD surface. Hence, this work strongly implies that free cholesterol localizing to the surface of LDs interferes with the functions of these metabolic proteins.

In summary, our current work sheds light on why adipocytes, the cellular fat reservoirs, store so little esterified cholesterol and further highlights the importance of adipocyte cholesterol on lipid droplet dynamics and caveolae function. Our work uncovers a unique aspect in the regulation of cholesterol homeostasis in adipocytes and suggests that increased ACAT proteins and activity may underpin certain adverse metabolic changes under pathological conditions such as extreme obesity. Therefore, ACAT inhibitors may be tested in treating disease conditions associated with extreme obesity.

## Experimental procedures

### Mice

C57BL/6J *ob*/*ob* mice and their age-matched WT control mice were maintained at 22 ± 1 °C with a 12-h light/dark cycle and *ad libitum* access to standard rodent chow and water. Epididymal adipose tissue was dissected from male mice (18–20 weeks old) and immediately snap frozen for later analysis. Ovarian adipose tissue was dissected from female animals (19–32 weeks old) and immediately used for adipocyte isolation. All procedures were approved by the Garvan Institute/St. Vincent's Hospital Animal Experimentation Ethics Committee and followed guidelines issued by the National Health and Medical Research Council of Australia.

### Adipocyte isolation

Ovarian fat pads dissected from mice were minced in 6-cm dishes. Digestion solution was freshly prepared by adding collagenase D (Sigma–Aldrich) (0.75 mg/ml), 0.901 mM $CaCl_2$, and 0.493 mM $MgCl_2$ in Dulbecco's PBS buffer. Minced fat pads were digested using 2 ml of digestion solution in 37 °C shaking water bath for 30 min. 10 ml of prewarmed DMEM (Life Technologies) medium was added to suspensions that were filtered through a 100-$\mu$m cell strainer (Falcon). After centrifugation at 700 × *g* for 5 min, mature adipocytes and stromal vascular fraction pellets were collected, respectively, for protein extraction.

### cDNA constructs

FLAG-tagged human ACAT1 and ACAT2 were subcloned into retroviral vector pBABE-puro using standard procedures. Primers were designed in-frame according to the multiple cloning site of pBABE-puro and are listed in Table S1. The catalytic dead ACAT1/2 (ACAT1-H460A and ACAT2-H360A) and ACAT2 stable mutants (ACAT2-C277A and ACAT2-H360A-C277A) were generated by a two-step site-directed mutagenesis (59). Site-directed mutagenesis primers were designed containing mutations of the corresponding amino acid change and are listed in Table S2. All constructs were verified by Sanger sequencing.

### Mammalian cell culture and transfection

HEK293FT and Phoenix Eco cells were cultured in high-glucose DMEM supplemented with 10% FBS (Life Technologies) and 1% penicillin/streptomycin/glutamine (PSG) (Life Technologies). 3T3-L1 cells were cultured in high-glucose DMEM supplemented with 10% newborn calf serum (Life Technologies) and 1% PSG. The cells were incubated at 37 °C with 5% $CO_2$, and the medium was changed every 2 days. DNA transfection was performed using Lipofectamine™ LTX and Plus reagent (Life Technologies) according to the manufacturer's instructions.

### Viral transduction

To generate stable cell lines or to transfect mature adipocytes, viral overexpressing constructs were transduced to target cells. Briefly, 2 × $10^6$ Phoenix Eco cells for retroviral overexpression or HEK293FT cells for lentiviral overexpression were seeded in 10-cm dishes 24 h prior to transfection. For retrovirus production 6 $\mu$g of pBABE-puro plasmids or for lentivirus production 10 $\mu$g of RRL-PGK plasmids together with 3 $\mu$g of pRSV (Rev), 2 $\mu$g of pMD.G (vesicular stomatitis virus), and 4 $\mu$g of pMDLg/pRRE (Gag/Pol) were transfected into target cells for 48 h. The viral medium was filtered through a 0.45-$\mu$m filter (Life Technologies) and collected into 15-ml falcon tubes. 8 $\mu$g/ml Polybrene (Sigma–Aldrich) was added to the filtered viral medium, which was then added to the target cells and incubated for 24–48 h. For mature adipocytes transduced with lentivirus, the cells were split and reseeded into different dishes depending on the experimental purposes. For the generation of stable cell lines transduced with retrovirus, the viral medium was refreshed to DMEM, 10% newborn calf serum, 1% PSG containing 4 $\mu$g/ml puromycin (Life Technologies) to select positively infected cells. The cells were selected for 72 h followed by a further 48 h.

### Cell treatments

The cells were grown to desired cell confluency using DMEM supplemented with serum and PSG depending on cell types. Insulin (10 nM) (Sigma–Aldrich), isoproterenol (10 $\mu$M) (Sigma–Aldrich), mevastatin (10 $\mu$M) (Sigma–Aldrich), HPCD (1% w/v) (Sigma–Aldrich), Sandoz 58-035 (10 $\mu$M) (Sigma–Aldrich), and PPPA (10 $\mu$M) (Cayman Chemical) (60, 61) were used in this study. The incubation time for each drug treatment is stated in the figure legends. To induce lipid droplet

formation, 200 $\mu$M oleate (Sigma–Aldrich) was added to preadipocytes for the indicated time.

### *RNA extraction and quantitative real-time PCR*

Total RNA was extracted using TRIzol™ reagent (Sigma–Aldrich). Mammalian cells were grown in 6-well plates. The cells were washed with PBS once and then lysed by the addition of 1 ml of TRIzol™ regent and incubation for 5 min at room temperature. 200 $\mu$l of chloroform (Sigma–Aldrich) was added to the lysates, shaking for 30 times violently, followed by incubation for 5 min at room temperature. The mixture was then centrifuged at 12,000 × *g* for 15 min at 4 °C. 350 $\mu$l of upper aqueous phase was carefully removed to a fresh tube, and the same volume of isopropanol (Sigma–Aldrich) was added and mixed well by the vortex for 5 s. The mixture was centrifuged at 12,000 × *g* for 10 min at 4 °C. After removing the upper aqueous phase, the pellet was washed twice with 1 ml of 75% ethanol (Sigma–Aldrich). The centrifugation of 7500 × *g* for 5 min at 4 °C was carried out between each wash. The RNA pellet was dried in fume hood after removing ethanol and then dissolved in RNase free water (Life Technologies). RNA concentration and purity were determined using Nanodrop spectrophotometer (Thermo Fisher Scientific). 1 $\mu$g of RNA was adopted for cDNA synthesis using the high-capacity cDNA reverse transcription kit (Thermal Fisher Scientific). Quantitative RT-PCR was performed with a Rotor-Gene 6000 real-time PCR machine (Qiagen) using KAPA SYBR® Green mix (KAPA Biosystems). The mRNA levels were normalized against the housekeeping gene and compared with control samples. All quantitative RT-PCR primers used in this study are listed in Table S3.

### *Antibodies*

We obtained rabbit polyclonal to HSL, p-HSL (Ser660), ATGL, perilipin2, AKT, $\beta$-Actin, GAPDH, and rabbit monoclonal to p-AKT (S473) from Cell Signaling Technology, goat polyclonal to perilipin-1, and rabbit polyclonal to ACAT1 (Abcam), mouse monoclonal to p-perilipin1 ($Ser^{522}$) (Vala Biosciences), rabbit polyclonal to ACAT2 (Cayman Chemical), caveolin-1 (Sigma–Aldrich), CD11b (Novus), FLAG (Clontech), and CIDEC (gift from Prof. Peng Li). All antibodies were diluted in 1:1000 except for ACAT1/2 at 1:500. For immunoblotting, we obtained horseradish peroxidase– conjugated secondary antibodies from Jackson ImmunoResearch. For immunofluorescence, we obtained Alexa Fluor– conjugated secondary antibodies from Molecular Probes/Life Technologies.

### *Immunoblot analysis*

The samples were mixed with 2× Laemmli buffer, incubated for 10–15 min at 70 °C, and then subjected to 10% SDS-PAGE. After electrophoresis, the proteins were transferred to Hybond-C nitrocellulose filters (GE Healthcare). Incubations with primary antibodies were performed at 4 °C overnight. Secondary antibodies were peroxidase-conjugated AffiniPure donkey anti-rabbit, donkey anti-mouse, or donkey anti-goat IgG (H+L; Jackson ImmunoResearch Laboratories) used at a 1:1000 dilution. The bound antibodies were detected by ECL Western blotting detection reagent (GE Healthcare or Merck Millipore) and visualized with Molecular Imager® ChemiDoc™ XRS+ (Bio-Rad).

### *Filipin staining*

The filipin complex (Sigma–Aldrich) was dissolved in DMSO (Sigma–Aldrich), and a working solution of 0.05 mg/ml in PBS containing 10% FBS was used. Cells grown on coverslips were rinsed with PBS three times and then fixed with 4% paraformaldehyde (PFA) (EM Science) for 15 min. After washing three times with PBS, the cells were incubated with 1 ml of glycine (Sigma–Aldrich) in PBS (1.5 mg/ml) for 10 min at room temperature to quench PFA. Then cells were stained with 1 ml of filipin working solution for 2 h in the dark at room temperature. When lipid droplets staining was required, 1 $\mu$g/ml BODIPY 493/503 (Life Technologies) or HCS LipidTOX™ deep red neutral lipid stain (1:500) (Life Technologies) was supplemented to the filipin working solution at the last 15 or 45 min depending on the dye used. The cells were mounted on the slides after rinsing with PBS three times.

### *Immunofluorescence*

Cells grown on coverslips were fixed with 4% PFA for 15 min and then permeabilized using 0.1% Triton X-100 (Sigma–Aldrich) in PBS for 30 min. The cells were washed with PBS three times and then blocked using 1% BSA (w/v) (Sigma–Aldrich) diluted in PBS for 1 h at 37 °C. After blocking, the cells were incubated with primary antibody at 4 °C overnight. The primary antibody was diluted in PBS at the ratio of 1:100. The cells were then washed three times in PBS before the incubation with the appropriate secondary Alexa Fluor antibody (Life Technologies) at 37 °C for 1 h. The secondary antibody was diluted in PBS at the ratio of 1:500. The coverslips were washed three times for 5 min each time in PBS and then mounted onto slides using ProLong® Antifade Gold reagent (Life Technologies) and sealed with nail polish. When filipin staining was required after immunofluorescence, the cells were permeabilized using 0.1% saponin (Sigma–Aldrich). All antibodies were diluted in 0.05% saponin. Confocal microscopy was performed using an Olympus FV1200 laser scanning confocal microscope (Olympus, Tokyo, Japan). A 100×/1.4 oil immersion objective was used for all imaging except for special specifications. The diameters of the LDs were measured using ImageJ software (National Institutes of Health).

### *Oil Red O staining*

3T3-L1 adipocytes grown in 6-well plates were washed with PBS once before fixed with 2 ml of 4% PFA for 1 h at room temperature. After fixing, 2 ml of 100% isopropanol (Ajax FineChem) was added to fixed cells. The plate was swirled to mix well. The mixture was removed and washed with 2 ml of 60% isopropanol (Ajax FineChem). After the removal of isopropanol, the plates were left to dry. 2 ml of Oil Red O (Sigma–Aldrich) solution was added and left to incubate for 10 min. The cells were then immediately washed with MilliQ $H_2O$ four times until all residual Oil Red O solution was removed. The plates were dried completely before imaging by a scanner.

### Lipolysis assay

3T3-L1 mature adipocytes overexpressing ACATs were split into 96-well plates. The lipolysis assay was carried out using the glycerol release assay kit (Biovision) according to the manufacturer's protocol with minor changes. To induce lipolysis, 75 $\mu$l of lipolysis assay medium was added to cells for indicated time points with 10 $\mu$M isoproterenol supplement. Glycerol standard was made using dilutions of glycerol in glycerol assay buffer. 50 $\mu$l of lipolysis assay medium was used to determine the glycerol released in samples. The reaction mixture was added to glycerol standards and samples and incubated for 30 min at room temperature protected from light. The reaction results were determined using a plate reader at 570 nm. Glycerol released from samples was normalized to the protein concentration of each sample.

### Neutral lipid extraction

After washing cells once with PBS, the neutral lipids were extracted by a 2-ml mixture of hexane (Ajax FineChem) and isopropanol (Ajax FineChem) (3:2) for 30 min in the fume hood. The solvent was then transferred into 2-ml glass vials. Another 1 ml of fresh hexane and isopropanol was used to collect the lipid residues in the dish and then transferred to glass vials together with the previous 2-ml solvent. The lipids were dried using a speed vacuum centrifuge. The cells were lysed with 0.1 M NaOH (Ajax FineChem) for 15 min at room temperature after the dish was dried. The protein concentrations were determined by bicinchoninic acid (Thermo Fisher Scientific) assay.

### Thin-layer chromatography

Neutral lipids were reconstituted in 60 $\mu$l of hexane. The samples were then loaded on and separated using a Silica Gel 60 plate (Millipore) and developed in a solvent system consisting of heptane/diethyl ether/glacial acetic acid (90:30:1) (Ajax FineChem). Separated lipids were stained with iodine for ~15 min. The TLC plate was scanned using the Epson Perfection 4490 Photo, and TAG bands were quantified using ImageJ software and normalized to the protein concentration.

### Cholesterol and cholesteryl ester measurement

Cholesterol was extracted using the same method as the neutral lipid extraction. The Amplex™ Red cholesterol assay kit (Life Technologies) was used to check the levels of free cholesterol and cholesteryl esters according to the manufacturer's protocol. Cholesterol-containing samples were diluted in an appropriate volume of 1× reaction buffer. Free cholesterol was measured by the enzyme-coupled reaction without cholesterol esterase. The cholesteryl esters were hydrolyzed into free cholesterol by cholesterol esterase and were then detected by subtracting free cholesterol from total cholesterol. The reactions were incubated for 30 min at 37 °C protected from light before measuring fluorescence using a microplate reader.

### Cholesterol esterification assay

3T3-L1 preadipocytes stably overexpressing ACAT1/2 were seeded in 6-cm dishes and grown to ~60–70% confluency. The cells were washed once using PBS, incubated with 2 ml of cholesterol-free medium (LPDS medium) overnight. The starvation medium was replaced by DMEM supplemented with 20% FBS for 5 h. [$^{14}$C]Oleic acid (1 $\mu$Ci) conjugated to BSA was then directly added to the medium, and the cells were chased for further 2 h. The cells were washed twice using buffer A (50 mM Tris-HCl, 150 mM NaCl, 0.2% (w/v) BSA, pH 7.4) and once with buffer B (50 mM Tris-HCl, 150 mM NaCl, pH 7.4). The liquid residues were removed completely. Lipid extraction and TLC were carried out as described above. The TLC plate was exposed to a BAS-MS imaging sheet (Fujifilm, Tokyo, Japan) for 5–7 days in an enclosed cassette at room temperature before visualizing the cholesteryl ester band using the FLA-5100 phosphorimaging device (Fujifilm). The relative intensities of bands corresponding to cholesteryl esters were quantified using ImageJ.

### Statistical analysis

All data were expressed as means ± S.D. or means ± S.E. Comparisons between two groups were analyzed using two-tailed Student's $t$ test or one-way analysis of variance using GraphPad Prism 6.0 software. Differences at values of $p < 0.05$ were considered to be significant.

*Author contributions*—Y. X., X. D., and H. Y. conceptualization; Y. X. and X. D. data curation; Y. X., X. D., and H. Y. formal analysis; Y. X., N. T., and H. Y. investigation; Y. X., N. T., A. J. B., and H. Y. methodology; X. D., A. J. B., and H. Y. writing-review and editing; A. J. B. and H. Y. supervision; H. Y. resources; H. Y. funding acquisition; H. Y. writing-original draft.

*Acknowledgment—We thank the Biomedical Imaging Facility at the University of New South Wales Mark Wainwright Analytical Centre, Australia.*

## References

1. Tabas, I. (2002) Consequences of cellular cholesterol accumulation: basic concepts and physiological implications. *J. Clin. Invest.* **110,** 905–911 CrossRef Medline
2. Brown, M. S., and Goldstein, J. L. (1997) The SREBP pathway: regulation of cholesterol metabolism by proteolysis of a membrane-bound transcription factor. *Cell* **89,** 331–340 CrossRef Medline
3. Sakakura, Y., Shimano, H., Sone, H., Takahashi, A., Inoue, N., Toyoshima, H., Suzuki, S., Yamada, N., and Inoue, K. (2001) Sterol regulatory element-binding proteins induce an entire pathway of cholesterol synthesis. *Biochem. Biophys. Res. Commun.* **286,** 176–183 CrossRef Medline
4. Horton, J. D., Goldstein, J. L., and Brown, M. S. (2002) SREBPs: activators of the complete program of cholesterol and fatty acid synthesis in the liver. *J. Clin. Invest.* **109,** 1125–1131 CrossRef Medline
5. Goldstein, J. L., and Brown, M. S. (2009) The LDL receptor. *Arterioscler. Thromb. Vasc. Biol.* **29,** 431–438 CrossRef Medline
6. DeBose-Boyd, R. A. (2008) Feedback regulation of cholesterol synthesis: sterol-accelerated ubiquitination and degradation of HMG CoA reductase. *Cell Res.* **18,** 609–621 CrossRef Medline
7. Gill, S., Stevenson, J., Kristiana, I., and Brown, A. J. (2011) Cholesterol-dependent degradation of squalene monooxygenase, a control point in cholesterol synthesis beyond HMG-CoA reductase. *Cell Metab.* **13,** 260–273 CrossRef Medline
8. Chang, T. Y., Li, B. L., Chang, C. C., and Urano, Y. (2009) Acyl-coenzyme A:cholesterol acyltransferases. *Am. J. Physiol. Endocrinol. Metab.* **297,** E1–E9 CrossRef Medline

9. Gao, M., Huang, X., Song, B. L., and Yang, H. (2019) The biogenesis of lipid droplets: lipids take center stage. *Prog. Lipid Res.* **75,** 100989 CrossRef Medline
10. Yang, H., Galea, A., Sytnyk, V., and Crossley, M. (2012) Controlling the size of lipid droplets: lipid and protein factors. *Curr. Opin. Cell Biol.* **24,** 509–516 CrossRef Medline
11. Walther, T. C., Chung, J., and Farese, R. V., Jr. (2017) Lipid droplet biogenesis. *Annu. Rev. Cell Dev. Biol.* **33,** 491–510 CrossRef Medline
12. Koivuniemi, A., Vuorela, T., Kovanen, P. T., Vattulainen, I., and Hyvönen, M. T. (2012) Lipid exchange mechanism of the cholesteryl ester transfer protein clarified by atomistic and coarse-grained simulations. *PLoS Comput. Biol.* **8,** e1002299 CrossRef Medline
13. Oelkers, P., Behari, A., Cromley, D., Billheimer, J. T., and Sturley, S. L. (1998) Characterization of two human genes encoding acyl coenzyme A:cholesterol acyltransferase-related enzymes. *J. Biol. Chem.* **273,** 26765–26771 CrossRef Medline
14. Farese, R. V., Jr. (1998) Acyl CoA:cholesterol acyltransferase genes and knockout mice. *Curr. Opin. Lipidol.* **9,** 119–123 CrossRef Medline
15. Cases, S., Novak, S., Zheng, Y. W., Myers, H. M., Lear, S. R., Sande, E., Welch, C. B., Lusis, A. J., Spencer, T. A., Krause, B. R., Erickson, S. K., and Farese, R. V., Jr. (1998) ACAT-2, a second mammalian acyl-CoA:cholesterol acyltransferase: its cloning, expression, and characterization. *J. Biol. Chem.* **273,** 26755–26764 CrossRef Medline
16. Lee, R. G., Willingham, M. C., Davis, M. A., Skinner, K. A., and Rudel, L. L. (2000) Differential expression of ACAT1 and ACAT2 among cells within liver, intestine, kidney, and adrenal of nonhuman primates. *J. Lipid Res.* **41,** 1991–2001 Medline
17. Sakashita, N., Miyazaki, A., Takeya, M., Horiuchi, S., Chang, C. C., Chang, T. Y., and Takahashi, K. (2000) Localization of human acyl-coenzyme A: cholesterol acyltransferase-1 (ACAT-1) in macrophages and in various tissues. *Am. J. Pathol.* **156,** 227–236 CrossRef Medline
18. Parini, P., Davis, M., Lada, A. T., Erickson, S. K., Wright, T. L., Gustafsson, U., Sahlin, S., Einarsson, C., Eriksson, M., Angelin, B., Tomoda, H., Omura, S., Willingham, M. C., and Rudel, L. L. (2004) ACAT2 is localized to hepatocytes and is the major cholesterol-esterifying enzyme in human liver. *Circulation* **110,** 2017–2023 CrossRef Medline
19. Nguyen, T. M., Sawyer, J. K., Kelley, K. L., Davis, M. A., and Rudel, L. L. (2012) Cholesterol esterification by ACAT2 is essential for efficient intestinal cholesterol absorption: evidence from thoracic lymph duct cannulation. *J. Lipid Res.* **53,** 95–104 CrossRef Medline
20. Rosen, E. D., and MacDougald, O. A. (2006) Adipocyte differentiation from the inside out. *Nat. Rev. Mol. Cell Biol.* **7,** 885–896 CrossRef Medline
21. Krause, B. R., and Hartman, A. D. (1984) Adipose tissue and cholesterol metabolism. *J. Lipid Res.* **25,** 97–110 Medline
22. Le Lay, S., Ferré, P., and Dugail, I. (2004) Adipocyte cholesterol balance in obesity. *Biochem. Soc. Trans.* **32,** 103–106 CrossRef Medline
23. Wang, M., Gao, M., Liao, J., Qi, Y., Du, X., Wang, Y., Li, L., Liu, G., and Yang, H. (2016) Adipose tissue deficiency results in severe hyperlipidemia and atherosclerosis in the low-density lipoprotein receptor knockout mice. *Biochim. Biophys. Acta* **1861,** 410–418 CrossRef Medline
24. Little, M. T., and Hahn, P. (1992) Ontogeny of acyl-CoA: cholesterol acyltransferase in rat liver, intestine, and adipose tissue. *Am. J. Physiol.* **262,** G599–G602 Medline
25. Prattes, S., Hörl, G., Hammer, A., Blaschitz, A., Graier, W. F., Sattler, W., Zechner, R., and Steyrer, E. (2000) Intracellular distribution and mobilization of unesterified cholesterol in adipocytes: triglyceride droplets are surrounded by cholesterol-rich ER-like surface layer structures. *J. Cell Sci.* **113,** 2977–2989 Medline
26. Parton, R. G., and del Pozo, M. A. (2013) Caveolae as plasma membrane sensors, protectors and organizers. *Nat. Rev. Mol. Cell Biol.* **14,** 98–112 CrossRef Medline
27. Weisberg, S. P., McCann, D., Desai, M., Rosenbaum, M., Leibel, R. L., and Ferrante, A. W., Jr. (2003) Obesity is associated with macrophage accumulation in adipose tissue. *J. Clin. Invest.* **112,** 1796–1808 CrossRef Medline
28. Wang, Y.-J., Bian, Y., Luo, J., Lu, M., Xiong, Y., Guo, S.-Y., Yin, H.-Y., Lin, X., Li, Q., Chang, C. C. Y., Chang, T.-Y., Li, B.-L., and Song, B.-L. (2017) Cholesterol and fatty acids regulate cysteine ubiquitylation of ACAT2 through competitive oxidation. *Nat. Cell Biol.* **19,** 808–819 CrossRef Medline
29. Sun, L., Nicholson, A. C., Hajjar, D. P., Gotto, A. M., Jr, and Han, J. (2003) Adipogenic differentiating agents regulate expression of fatty acid binding protein and CD36 in the J744 macrophage cell line. *J. Lipid Res.* **44,** 1877–1886 CrossRef Medline
30. Farmer, S. R. (2006) Transcriptional control of adipocyte formation. *Cell Metab.* **4,** 263–273 CrossRef Medline
31. Hudak, C. S., and Sul, H. S. (2013) Pref-1, a gatekeeper of adipogenesis. *Front. Endocrinol.* (*Lausanne*) **4,** 79 CrossRef Medline
32. Nishino, N., Tamori, Y., Tateya, S., Kawaguchi, T., Shibakusa, T., Mizunoya, W., Inoue, K., Kitazawa, R., Kitazawa, S., Matsuki, Y., Hiramatsu, R., Masubuchi, S., Omachi, A., Kimura, K., Saito, M., *et al.* (2008) FSP27 contributes to efficient energy storage in murine white adipocytes by promoting the formation of unilocular lipid droplets. *J. Clin. Invest.* **118,** 2808–2821 Medline
33. Gong, J., Sun, Z., Wu, L., Xu, W., Schieber, N., Xu, D., Shui, G., Yang, H., Parton, R. G., and Li, P. (2011) Fsp27 promotes lipid droplet growth by lipid exchange and transfer at lipid droplet contact sites. *J. Cell Biol.* **195,** 953–963 CrossRef Medline
34. Grahn, T. H., Kaur, R., Yin, J., Schweiger, M., Sharma, V. M., Lee, M. J., Ido, Y., Smas, C. M., Zechner, R., Lass, A., and Puri, V. (2014) Fat-specific protein 27 (FSP27) interacts with adipose triglyceride lipase (ATGL) to regulate lipolysis and insulin sensitivity in human adipocytes. *J. Biol. Chem.* **289,** 12029–12039 CrossRef Medline
35. Murphy, D. J., and Vance, J. (1999) Mechanisms of lipid-body formation. *Trends Biochem. Sci.* **24,** 109–115 CrossRef Medline
36. Buhman, K. K., Chen, H. C., and Farese, R. V., Jr. (2001) The enzymes of neutral lipid synthesis. *J. Biol. Chem.* **276,** 40369–40372 CrossRef Medline
37. Miyoshi, H., Souza, S. C., Zhang, H. H., Strissel, K. J., Christoffolete, M. A., Kovsan, J., Rudich, A., Kraemer, F. B., Bianco, A. C., Obin, M. S., and Greenberg, A. S. (2006) Perilipin promotes hormone-sensitive lipase-mediated adipocyte lipolysis via phosphorylation-dependent and -independent mechanisms. *J. Biol. Chem.* **281,** 15837–15844 CrossRef Medline
38. Granneman, J. G., Moore, H. P., Krishnamoorthy, R., and Rathod, M. (2009) Perilipin controls lipolysis by regulating the interactions of AB-hydrolase containing 5 (Abhd5) and adipose triglyceride lipase (Atgl). *J. Biol. Chem.* **284,** 34538–34544 CrossRef Medline
39. Dimitriadis, G., Mitrou, P., Lambadiari, V., Maratou, E., and Raptis, S. A. (2011) Insulin effects in muscle and adipose tissue. *Diabetes Res. Clin. Pract.* **93,** S52–59 CrossRef Medline
40. Lam, Y. Y., Janovska, A., McAinch, A. J., Belobrajdic, D. P., Hatzinikolas, G., Game, P., and Wittert, G. A. (2011) The use of adipose tissue-conditioned media to demonstrate the differential effects of fat depots on insulin-stimulated glucose uptake in a skeletal muscle cell line. *Obes. Res. Clin. Pract.* **5,** e1–e78 CrossRef Medline
41. Fielding, C. J., and Fielding, P. E. (2000) Cholesterol and caveolae: structural and functional relationships. *Biochim. Biophys. Acta* **1529,** 210–222 CrossRef Medline
42. Liu, P., Rudick, M., and Anderson, R. G. (2002) Multiple functions of caveolin-1. *J. Biol. Chem.* **277,** 41295–41298 CrossRef Medline
43. Le Lay, S., Hajduch, E., Lindsay, M. R., Le Lièpvre, X., Thiele, C., Ferré, P., Parton, R. G., Kurzchalia, T., Simons, K., and Dugail, I. (2006) Cholesterol-induced caveolin targeting to lipid droplets in adipocytes: a role for caveolar endocytosis. *Traffic* **7,** 549–561 CrossRef Medline
44. Qin, L., Zhu, N., Ao, B. X., Liu, C., Shi, Y. N., Du, K., Chen, J. X., Zheng, X. L., and Liao, D. F. (2016) Caveolae and caveolin-1 integrate reverse cholesterol transport and inflammation in atherosclerosis. *Int. J. Mol. Sci.* **17,** 429 CrossRef Medline
45. Krishna, A., and Sengupta, D. (2019) Interplay between membrane curvature and cholesterol: role of palmitoylated caveolin-1. *Biophys. J.* **116,** 69–78 CrossRef Medline
46. Zhu, Y., Chen, C. Y., Li, J., Cheng, J. X., Jang, M., and Kim, K. H. (2018) *In vitro* exploration of ACAT contributions to lipid droplet formation during adipogenesis. *J. Lipid Res.* **59,** 820–829 CrossRef Medline

47. Temel, R. E., Hou, L., Rudel, L. L., and Shelness, G. S. (2007) ACAT2 stimulates cholesteryl ester secretion in apoB-containing lipoproteins. *J. Lipid Res.* **48,** 1618–1627 CrossRef Medline
48. Brown, J. M., Bell, T. A., 3rd, Alger, H. M., Sawyer, J. K., Smith, T. L., Kelley, K., Shah, R., Wilson, M. D., Davis, M. A., Lee, R. G., Graham, M. J., Crooke, R. M., and Rudel, L. L. (2008) Targeted depletion of hepatic ACAT2-driven cholesterol esterification reveals a non-biliary route for fecal neutral sterol loss. *J. Biol. Chem.* **283,** 10522–10534 CrossRef Medline
49. Zhang, J., Kelley, K. L., Marshall, S. M., Davis, M. A., Wilson, M. D., Sawyer, J. K., Farese, R. V., Jr, Brown, J. M., and Rudel, L. L. (2012) Tissue-specific knockouts of ACAT2 reveal that intestinal depletion is sufficient to prevent diet-induced cholesterol accumulation in the liver and blood. *J. Lipid Res.* **53,** 1144–1152 CrossRef Medline
50. Fang, S., Ferrone, M., Yang, C., Jensen, J. P., Tiwari, S., and Weissman, A. M. (2001) The tumor autocrine motility factor receptor, gp78, is a ubiquitin protein ligase implicated in degradation from the endoplasmic reticulum. *Proc. Natl. Acad. Sci. U.S.A.* **98,** 14422–14427 CrossRef Medline
51. Sever, N., Song, B. L., Yabe, D., Goldstein, J. L., Brown, M. S., and DeBose-Boyd, R. A. (2003) Insig-dependent ubiquitination and degradation of mammalian 3-hydroxy-3-methylglutaryl-CoA reductase stimulated by sterols and geranylgeraniol. *J. Biol. Chem.* **278,** 52479–52490 CrossRef Medline
52. Song, B. L., Sever, N., and DeBose-Boyd, R. A. (2005) Gp78, a membrane-anchored ubiquitin ligase, associates with Insig-1 and couples sterol-regulated ubiquitination to degradation of HMG CoA reductase. *Mol. Cell* **19,** 829–840 CrossRef Medline
53. Song, B. L., and DeBose-Boyd, R. A. (2006) Insig-dependent ubiquitination and degradation of 3-hydroxy-3-methylglutaryl coenzyme a reductase stimulated by delta- and gamma-tocotrienols. *J. Biol. Chem.* **281,** 25054–25061 CrossRef Medline
54. Baumann, N. A., Sullivan, D. P., Ohvo-Rekilä, H., Simonot, C., Pottekat, A., Klaassen, Z., Beh, C. T., and Menon, A. K. (2005) Transport of newly synthesized sterol to the sterol-enriched plasma membrane occurs via nonvesicular equilibration. *Biochemistry* **44,** 5816–5826 CrossRef Medline
55. Mesmin, B., and Antonny, B. (2016) The counterflow transport of sterols and PI4P. *Biochim. Biophys. Acta* **1861,** 940–951 CrossRef Medline
56. Wong, L. H., Copic, A., and Levine, T. P. (2017) Advances on the transfer of lipids by lipid transfer proteins. *Trends Biochem. Sci.* **42,** 516–530 CrossRef Medline
57. Wang, H., Ma, Q., Qi, Y., Dong, J., Du, X., Rae, J., Wang, J., Wu, W. F., Brown, A. J., Parton, R. G., Wu, J. W., and Yang, H. (2019) ORP2 delivers cholesterol to the plasma membrane in exchange for phosphatidylinositol 4,5-Bisphosphate (PI(4,5)P2). *Mol. Cell* **73,** 458–473.e7 CrossRef Medline
58. Hynynen, R., Suchanek, M., Spandl, J., Bäck, N., Thiele, C., and Olkkonen, V. M. (2009) OSBP-related protein 2 is a sterol receptor on lipid droplets that regulates the metabolism of neutral lipids. *J. Lipid Res.* **50,** 1305–1315 CrossRef Medline
59. Du, X., Kumar, J., Ferguson, C., Schulz, T. A., Ong, Y. S., Hong, W., Prinz, W. A., Parton, R. G., Brown, A. J., and Yang, H. (2011) A role for oxysterol-binding protein-related protein 5 in endosomal cholesterol trafficking. *J. Cell Biol.* **192,** 121–135 CrossRef Medline
60. Lada, A. T., Davis, M., Kent, C., Chapman, J., Tomoda, H., Omura, S., and Rudel, L. L. (2004) Identification of ACAT1- and ACAT2-specific inhibitors using a novel, cell-based fluorescence assay: individual ACAT uniqueness. *J. Lipid Res.* **45,** 378–386 CrossRef Medline
61. Guo, D., Zhang, X., Li, Q., Qian, L., Xu, J., Lu, M., Hu, X., Zhu, M., Chang, C. C., Song, B., Chang, T., Xiong, Y., and Li, B. (2016) The ACAT2 expression of human leukocytes is responsible for the excretion of lipoproteins containing cholesteryl/steryl esters. *Acta Biochim. Biophys. Sin.* (*Shanghai*) **48,** 990–997 CrossRef Medline